

Heparanase Regulates Murine Hair Growth

Eyal Zcharia,* Deborah Philp,[†] Evgeny Edovitsky,*
Helena Aingorn,* Shula Metzger,[‡]
Hynda K. Kleinman,[†] Israel Vlodavsky,[§] and
Michael Elkin*

From the Departments of Oncology* and Internal Medicine,[‡]
Hadassah-Hebrew University Medical Center, Jerusalem, Israel;
the Cancer and Vascular Biology Research Center,[§] Bruce
Rappaport Faculty of Medicine, Technion, Haifa, Israel; and the
Cell Biology Section,[†] National Institute of Dental and
Craniofacial Research, National Institutes of Health,
Bethesda, Maryland

Heparanase is an endoglycosidase that cleaves heparan sulfate, the main polysaccharide component of the extracellular matrix. Heparan sulfate moieties are responsible for the extracellular matrix barrier function, as well as for sequestration of heparin-binding growth factors in the extracellular matrix. Degradation of heparan sulfate by heparanase enables cell movement through extracellular barriers and releases growth factors from extracellular matrix depots, making them bioavailable. Here, we demonstrate a highly coordinated temporospatial pattern of heparanase expression and enzymatic activity during hair follicle cycling. This pattern paralleled the route and timing of follicular stem cell progeny migration and reconstitution of the lower part of the follicle, which is a prerequisite for hair shaft formation. By monitoring *in vivo* activation of luciferase reporter gene driven by heparanase promoter, we observed activation of heparanase gene transcription at a specific stage of the hair cycle. Heparanase was produced by rat vibrissa bulge keratinocytes, closely related to a follicular stem cell population. Heparanase contributed to the ability of the bulge-derived keratinocytes to migrate through the extracellular matrix barrier *in vitro*. In heparanase-overexpressing transgenic mice, increased levels of heparanase enhanced active hair growth and enabled faster hair recovery after chemotherapy-induced alopecia. Collectively, our results identify heparanase as an important regulator of hair growth and suggest that cellular mechanisms of its action involve facilitation of follicular stem cell progeny migration and release of extracellular matrix-resident, heparin-bound growth factors, thus regulating hair cycle. (Am J Pathol 2005, 166:999–1008)

The hair follicle repeatedly undergoes phases of active hair shaft production (anagen), regression (catagen), and rest (telogen) throughout the life of mammals.^{1,2} The unique ability of the follicle to constantly renew is maintained by the multipotent keratinocyte stem cells, which generate differentiated progeny for the new hair shaft formation.^{1,3–6} The mature follicle is composed of two concentric layers of epithelial cells (keratinocytes), encircling the hair shaft and defined as inner and outer root sheaths (IRS and ORS).¹ The bulge region of the ORS, located close to the insertion of the arrector pili muscle, has been identified as a niche for the follicular stem cells.^{3–5,7,8} At the onset of anagen, some of the bulge-localized stem cells give rise to rapidly dividing transit-amplifying (TA) cells that migrate downward, reconstitute the lower part of the follicle, and further differentiate into the hair matrix cells, producing a new hair shaft.^{3,4,7,9} It is well established that the migratory behavior of different cell types in a variety of biological processes involves enzymatic degradation of the extracellular matrix (ECM), which represents the main physical barrier for cell movement.^{10,11} Similarly, cell migration in the follicular ORS involves ECM degradation. It was recently demonstrated that activity of the ECM-degrading enzyme matrix metalloproteinase 2 is required for migration of ORS-resident melanocyte precursors.¹² Likewise, TA cells, migrating during the anagen phase along the ORS, must degrade ECM barriers to move from the bulge region to the base of the follicle.

Heparan sulfate is the principal polysaccharide component of the ECM, and the basement membrane^{13,14} (specialized ECM structure that separates the ORS from the adjacent connective tissue sheath^{15,16}). Heparan sulfate molecules are long, highly sulfated linear carbohydrate chains linked to a core protein and unique in their ability to interact, via specific binding sites, with the protein constituents of the ECM.^{13,14} These interactions make heparan sulfate an essential molecule responsible

Supported by the Israel Science Foundation (grant 532/02); the Dalia Greidinger Fund; and the National Cancer Institute, National Institutes of Health (Public Health Service grant RO1-CA106456-01).

E.Z., D.P., and E.E. contributed equally to this work.

Accepted for publication December 16, 2004.

Address reprint requests to Israel Vlodavsky, Ph.D., Cancer and Vascular Biology Research Center, The Bruce Rappaport Faculty of Medicine, Technion, P. O. Box 9649, Haifa 31096, Israel. E-mail: vlodavsk@cc.huji.ac.il.

for the ECM barrier function.¹⁷ Another important characteristic of heparan sulfate moieties in the basement membrane and ECM is the ability to bind specifically various members of the heparin-binding growth factor family and to serve as their extracellular reservoir.^{18–21} Many heparan sulfate-bound growth factors, implicated in hair growth and differentiation (ie, hepatocyte growth factor, fibroblast growth factor, keratinocyte growth factor, vascular endothelial growth factor)^{2,22} are sequestered in the ECM and could be released by means of enzymatic cleavage of heparan sulfate.^{10,17,19,21,23,24}

Heparanase is the predominant mammalian enzyme capable of heparan sulfate degradation.^{10,25} Heparanase is expressed by cells of epithelial origin, endothelial cells, and activated cells of the immune system in various pathological conditions as well as in normal development.^{10,25,26} Previous studies have demonstrated that degradation of heparan sulfate by heparanase enables cell movement through extracellular barriers and releases heparan sulfate-bound growth factors from ECM depots, making them available for growth factor-dependent processes.^{10,26–28} In hair growth and cycling, the above aspects, namely cell motility and involvement of heparan sulfate-bound growth factors (eg, hepatocyte growth factor, fibroblast growth factor, keratinocyte growth factor, vascular endothelial growth factor) play critical roles.^{2,4,5,21,29}

We have observed an enhanced hair regrowth in the recently established heparanase-overexpressing transgenic (*hpa-tg*) mouse.³⁰ This observation prompted us to investigate the involvement of heparanase in hair growth, using *in vitro* and *in vivo* experimental systems. We demonstrated a highly coordinated temporospatial pattern of heparanase promoter activation, expression and enzymatic activity during hair follicle cycling. We report that bulge-derived clonogenic keratinocytes, representing a progeny of the follicular stem cells (ie, TA cells),^{5,31,32} produce heparanase. Using heparanase inhibitors and recombinant enzyme, we demonstrate that heparanase contributes to the ability of the clonogenic keratinocytes to migrate through an ECM barrier *in vitro*. In the *hpa-tg* mouse, increased levels of heparanase enhanced the active growth phase of the first postnatal hair cycle and the subsequent growth cycles, as well as enabled faster hair regrowth after chemotherapy-induced alopecia. Taken together, our results demonstrate that heparanase plays an important role in hair growth, and suggest that the cellular mechanism of its action may involve facilitation of follicular TA cell migration, as well as release of ECM-resident, heparan sulfate-bound growth factors, that regulate hair cycle.

Materials and Methods

Induction of Hair Cycle

Depilation was used to induce hair growth in resting follicles, as described.³³ The dorsal skin of 8-week-old female C57BL/6 mice at the telogen phase (as identified by their pink skin color) was depilated using Hair Remover Wax Strip kit (Del Laboratories, Farmingdale, NY),

leading to the synchronized development of anagen hair follicles. Skin tissue samples were collected on days 0, 4, and 9 after depilation; five mice per time point. The samples were fixed in 4% paraformaldehyde and processed for histological examination and immunostaining. The distinct hair cycle phases were determined as described.³⁴ For skin tissue lysate preparation, skin samples were snap-frozen in liquid nitrogen and pulverized to a fine powder with a liquid nitrogen-cooled pestle. The powder was resuspended in 2 ml of ice-cold lysis buffer containing 10 mmol/L phosphate-citrate, pH 6.0, 150 mmol/L NaCl, 1 mmol/L MgCl₂, 0.1 mmol/L ZnCl₂, and 0.5% Nonidet P-40, frozen, and thawed three times and centrifuged for 20 minutes at 4°C at 14,000 rpm. Lysate protein content was then determined.

First Physiological Postnatal Hair Cycle

Skin samples were obtained from *hpa-tg* and control wild-type newborn female mice at postnatal days 8, 12, 16, and 20 (two to three mice per each time point). Rectangular pieces of the central dorsal skin were collected parallel to the vertebral line, fixed in 4% paraformaldehyde, and processed for histological examination. Distinct stages of follicle morphogenesis were determined as described.³⁵ Cutaneous thickness (dermis + subcutis) was measured in digital images of hematoxylin and eosin-stained sections using the Scion software (Scion Cor., Frederick, MD). Sections from three animals per time point were used and 10 measurements per section were performed. Statistical analyses were performed using InStat software (Graph Pad Software, San Diego, CA).

Chemotherapy-Induced Alopecia

Anagen was induced in the back skin of mice in the telogen phase of the hair cycle, as described above. CYP-induced alopecia was induced as described,³⁶ with minor modifications. Briefly, on days 9 and 12 after depilation, CYP was injected intraperitoneally (125 mg per kg bodyweight). By day 15 after depilation, the mice exhibited complete alopecia on the previously depilated skin area (the loose hair shafts were removed from this area by 10 strokes backward and forward with a gloved finger). Skin tissue samples were collected on day 15 and day 30 after depilation (two to three mice per time point). The samples were fixed in 4% paraformaldehyde and processed for histological examination.

Immunohistochemistry

Immunohistochemistry was performed as described²⁵ with minor modifications. Briefly, 5- μ m sections of paraffin-embedded skin samples were deparaffinized and rehydrated. Tissue was then incubated in 3% H₂O₂, denatured by boiling (3 minutes) in a microwave oven in citrate buffer (0.01 mol/L, pH 6.0), and blocked with 10% goat serum in phosphate-buffered saline (PBS). Sections were incubated with specific polyclonal anti-heparanase anti-

bodies, raised against synthetic peptides 158 KKFKN-STYRSSVD 171 (no. 733) 37 and 273 RKTAKMLKSLKAG-GEVI 290 (both located in the 50-kd subunit of the active heparanase enzyme), diluted 1:100 in 10% goat serum in PBS, or with 10% goat serum alone, as a control. Color was developed by using the Zymed AEC substrate kit (Zymed Laboratories, South San Francisco, CA) for 10 minutes, followed by counterstaining with Mayer's hematoxylin.

Reporter Constructs and *In Vivo* Electroporation

The 1.9-kb human heparanase promoter region [Hpse (-1791/+109)-LUC] was subcloned upstream of the luciferase (LUC) gene in a pGL2 basic reporter plasmid (Promega, Madison, WI), as described. 38 The plasmid containing the LUC gene driven by the CMV enhancer/promoter (CMV-LUC) was a gift from Dr. A. Oppenheim (Hadassah-Hebrew University Hospital, Jerusalem, Israel).

For *in vivo* electroporation, mice were anesthetized and plasmid DNA (CMV-LUC and HPSE-LUC) was intradermally injected with a 0.3-ml syringe and 30-gauge needle into the upper and lower dorsal site, respectively (20 μ g per site in 25 μ l of PBS). To keep variability to a minimum, the same skilled operator performed all injections. A 30-second time interval lapsed between injection and initiation of electroporation. The *in vivo* electroporation system (Genetronics Inc., San Diego, CA) consisted of a square wave pulse generator (ECM 830) and a caliper electrode, applied topically. The caliper electrode (modes 384; BTX/Harvard Apparatus, Holliston, MA) consists of two 1-cm 2 brass plate electrodes, which squeeze the skin fold to be electroporated as described by Zhang and colleagues. 39 Electroporation was performed with 75 V; pulse length 20 msec, six pulses with an interval of 1 second, polarity reversal after three pulses.

In Vivo Imaging

The cooled-charged-coupled device (CCCD) camera model LN/CCD-1300EB equipped with ST-133 controller and a 50-mm Nikon lens (Roper Scientific, Princeton Instrument, Trenton, NJ), supported with comparable software was used for light detection, as described. 40 In this system, a pseudocolor image represents light intensity (least intense blue and most intense red). In all cases, the integrated light is the result of a 2-minute exposure and acquisition. In all experiments animals were anesthetized before light detection. The exposure conditions (including exposure time, distance of lens from the objects, and time after injection of luciferin) were kept identical. Ten minutes before monitoring light emission, the animals were injected intraperitoneally with Beetle luciferin (Promega Corp., Madison, WI) in PBS at 126 mg/kg body weight. Animals were placed in a dark box, supplemented with a controlled light to take pictures of the background gray-scale image and then exposed to the CCD, to generate a pseudo-color image that represents light intensity. For co-localization of the bioluminescent emission on the animal body, gray-scale and pseudo-color images were merged by using the appropriate im-

aging software. The Institutional Animal Care and Use Committee approved all procedures. Two animals per time point were used, yielding similar results. Representative results of one animal are shown.

Isolation of Clonogenic Keratinocytes

Clonogenic keratinocytes were isolated from Fisher 344 rat vibrissa follicles, as described. 32 After sacrifice, the upper lip containing the vibrissal pad was cut and vibrissa follicles were dissected and plucked from the pad under a dissecting microscope. A fragment of the follicle containing the bulge region was cut off and incubated for 30 minutes in collagenase/dispase solution (1 mg/ml; Roche Molecular Biochemicals, Indianapolis, IN) at 37°C. The epithelial core was detached from the collagen capsule and further incubated in 0.05% trypsin/collagenase/dispase solution (30 minutes, 37°C) to facilitate the dissociation of epithelial cells. Isolated cells were cultured in keratinocyte-serum-free medium (Keratinocyte-SFM) (Invitrogen, Carlsbad, CA), containing epidermal growth factor (2.5 μ g/500 ml), bovine pituitary extract (25 mg/500 ml), and 10% fetal calf serum. The seeding density was 1000 cells/35-mm plate, and 60 to 80 colonies per plate were formed by day 7 to 9 of culture. To characterize the pattern of keratin expression, the cells were lysed by the addition of RIPA buffer, and equal protein aliquots of cell lysates were separated on 4 to 12% Bis-Tris NuPAGE gels (Invitrogen). Proteins were transferred to a nitrocellulose membrane (Invitrogen). The same membrane has been reprobed using polyclonal antibodies against mouse keratins 5, 10, 14, and 15 (Covance Research Products, Richmond, CA). Clonogenic keratinocytes isolated in three independent experiments were tested and a similar pattern of keratin expression was detected.

Heparanase Activity

For measurements of heparanase enzymatic activity, tissue or cell lysates were incubated on dishes coated with sulfate-labeled ECM, prepared as described. 10,41 Briefly, bovine corneal endothelial cells were established and cultured at 37°C in a 10% CO $_2$ humidified incubator in Dulbecco's modified Eagle's medium (1 g of glucose/L) supplemented with 10% calf serum (Life Technologies, Grand Island, NY) and 5% dextran T-40 in the presence of Na $_2$ [35 S]O $_4$ (25 μ Ci/ml) (Amersham Pharmacia Biotech, Buckinghamshire, UK), added on days 1 and 5 after seeding. 10,41 The subendothelial ECM was exposed by dissolving the cell layer with PBS containing 0.5% Triton X-100 and 20 mmol/L NH $_4$ OH, followed by four washes in PBS. 10,41 Equal protein aliquots of tissue or cell lysates were incubated with the labeled ECM for 16 to 36 hours (37°C, pH 6.2). Sulfate-labeled material released into the incubation medium was analyzed by gel filtration on a Sepharose 6B column. 10,41 Nearly intact heparan sulfate proteoglycans are eluted just after the void volume (peak I, K_{av} < 0.2, fractions 1 to 10) and heparan sulfate deg-

radiation fragments are eluted later with $0.5 < K_{av} < 0.8$ (peak II, fractions 15 to 35).^{10,41}

Migration through Matrigel

Migration was studied in 48-well Boyden chambers using 8- μ m-pore polycarbonate membranes (Poretics, Livermore, CA) coated with 0.5 mg/ml of Matrigel (BD Biosciences, Bedford, MA) diluted in keratinocyte-SFM. The bottom chambers were filled with complete growth medium, containing epidermal growth factor (2.5 μ g/500 ml), bovine pituitary extract (25 mg/500 ml) (Invitrogen), and 10% fetal calf serum. Cultured clonogenic keratinocytes were harvested using trypsin and resuspended in keratinocyte-SFM containing 1% bovine serum albumin factor-V and 25 mmol/L HEPES-buffer. Some cells were either preincubated for 15 minutes with 5 μ g/ml recombinant heparanase enzyme (kindly provided by Dr. H.-Q. Miao, ImClone Inc., New York, NY) or mixed with the heparanase inhibitor laminaran sulfate (purchased from Qingdao Third Pharmaceutical Company, Qingdao, China). The cells (30,000 cells/well) were then added to the upper chambers and were incubated at 37°C and 5% CO₂ for 6 hours. The membranes were then fixed and stained with Diff-Quik (VWR, Bridgeport, NJ). Cell migration was quantitated in five random microscopic fields ($\times 100$) of triplicate wells. The assay was repeated twice.

Motility

Clonogenic keratinocytes were plated into 35-mm dishes. Migration was monitored for 20 hours using a Zeiss inverted microscope. Digital images were collected using a CCD camera (model 2400; Hamamatsu Photonics) at 10-minute intervals, stored as image stacks, converted to QuickTime movies and analyzed using MetaMorph Group 3.5 software (Universal Imaging Corp., London, UK). This experiment was repeated twice, six cells were tracked in each experiment.

Results

Heparanase Expression during the Hair Follicle Growth Cycle

We first explored the spatial and temporal patterns of endogenous heparanase expression in full-thickness skin samples collected during depilation-induced, synchronized adult hair cycling in C57BL/6J female mice. Immunohistochemical staining revealed no heparanase expression in telogen skin, as well as at early stages of the telogen-anagen transition (Figure 1, a and b). Heparanase protein was first detected in the ORS keratinocytes of elongating early anagen follicles (anagen III, 4 days after depilation), traversing dermis-subcutis boundaries and invading into subcutaneous tissue layers (Figure 1c, inset). Heparanase expression was confined to the keratinocytes located in the ORS portion under the bulge

(Figure 1c, inset) and persisted during the subsequent anagen stages (anagen III to VI; Figure 1, d to f). In addition, skin samples, harvested from newborn C57BL/6J mice in a course of the first postnatal hair cycle, were evaluated for heparanase expression. Similar to the pattern revealed during depilation-induced hair cycle, heparanase expression was observed through the stages of postnatal hair development, morphologically identical to early-mid anagen of later cycles, and down-regulated during the subsequent catagen-telogen (not shown). In telogen-anagen transition of the following cycle (postnatal day 28) no heparanase staining was detected (not shown). Interestingly, heparanase expression was mainly noted in the ORS areas along the hypothesized migration route of the TA cells (daughters of follicular keratinocyte stem cells),⁴ which emanate from the bulge and migrate downward to repopulate the lower follicle and the hair matrix cell compartment. Heparanase was absent in the matrix cells in the bulge region, suggesting correlation between migratory behavior and levels of the enzyme expression.

We next determined the levels of heparanase enzymatic activity in lysates of the mouse skin samples, harvested at defined phases of synchronized depilation-induced hair growth, to verify the immunostaining observations (Figure 1g). Heparanase activity was tested by incubation (16 hours, 37°C) of skin lysate with a metabolically sulfate-labeled ECM. Sulfate-labeled degradation products released into the incubation medium were subjected to gel filtration on Sepharose 6B columns.^{25,41} The substrate alone consisted almost entirely of nearly intact, high-molecular weight material eluted just after the void volume (peak I, fractions 1 to 10, $K_{av} < 0.2$). This material (peak I) has been previously shown to be generated by a proteolytic activity residing in the ECM itself and/or expressed by the cells.⁴² The elution pattern of labeled material released during incubation of the telogen skin lysate with sulfate-labeled ECM showed only a weak heparanase enzymatic activity, attributed primarily to the presence of residual heparanase-expressing blood cells (ie, platelets, lymphocytes, neutrophils)⁴² in the skin samples (Figure 1g). In contrast, a high heparanase activity was detected in lysates from anagen skin, resulting in release of 60 to 70% of the ECM-associated radioactivity in the form of low-molecular weight sulfate-labeled fragments (peak II, fractions 15 to 33, $0.5 < K_{av} < 0.8$) (Figure 1g).^{25,41} Labeled fragments eluted in peak II were shown to be degradation products of heparan sulfate because they were fivefold to sixfold smaller than intact heparan sulfate side chains, resistant to further digestion with papain and chondroitinase ABC, and susceptible to deamination by nitrous acid.⁴¹ These data indicate tight regulation of heparanase expression during the hair growth cycle. Moreover, the similarity between the spatiotemporal distribution of heparanase-expressing ORS keratinocytes and the hypothesized distribution of TA cells, emanating from the bulge cell compartment and repopulating the lower, cycling part of the follicle at the onset of anagen,^{3,4,7,9} suggests involvement of the enzyme in this process.

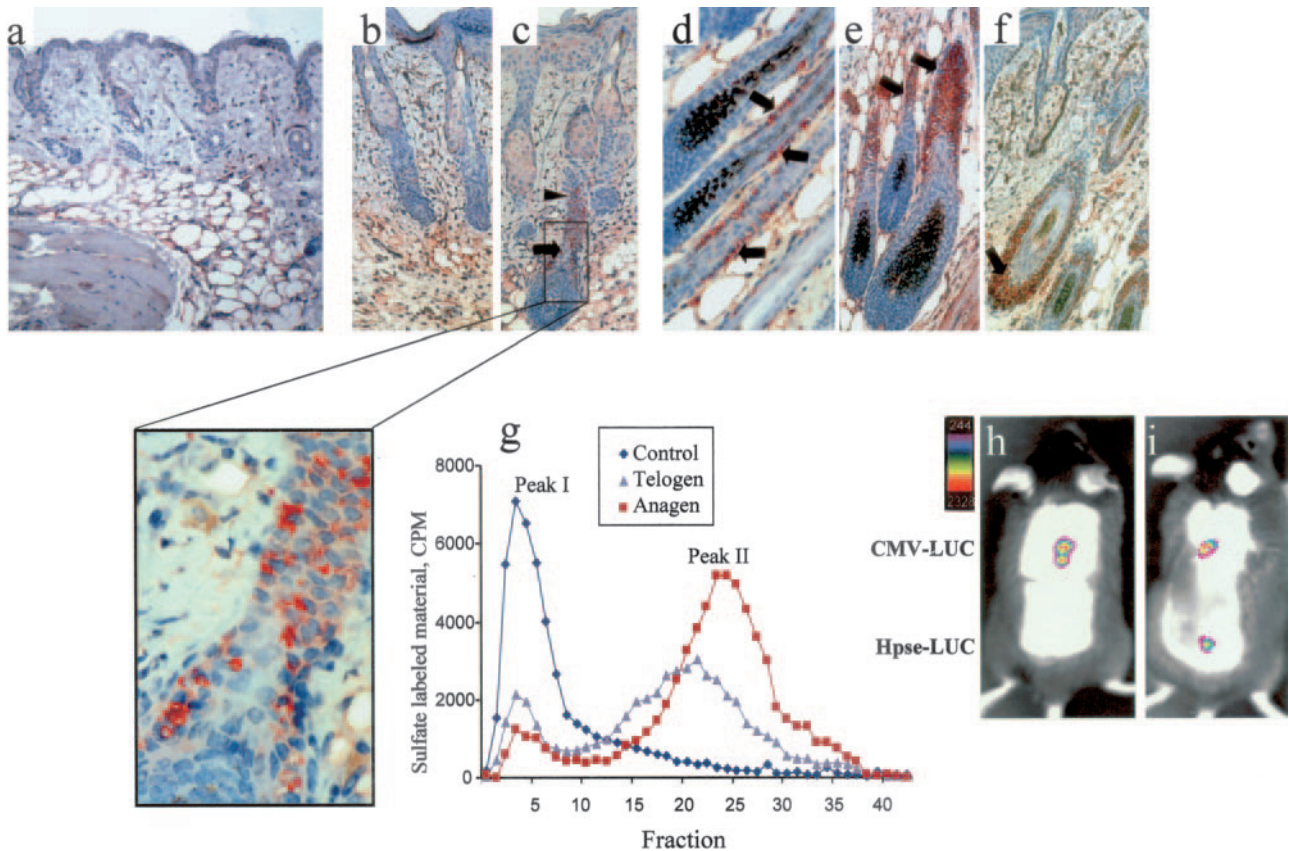


Figure 1. Heparanase expression during depilation-induced hair growth cycle. Dorsal skin of 7-week-old female C57BL/6 mouse was harvested at defined phases of the hair cycle (telogen, day 0, unmanipulated skin; early anagen, 4 days after depilation; and peak anagen, 9 days after depilation) and processed for histology (a–f) and tissue lysate preparation (g). a–f: Immunohistochemical analysis of heparanase expression (anti-heparanase antibody no. 733, reddish staining). Telogen skin: no heparanase-positive cells are detected in the follicles (a). Early anagen: heparanase expression is still absent in follicles residing entirely in the dermis (b) and begins in ORS keratinocytes (arrow) of the follicle traversing the dermis/subcutis boundaries and invading into the subcutaneous tissue (c, inset). Arrowhead: bulge region. Peak anagen skin: longitudinal (d, e) and transverse (f) sections of the follicle: heparanase-expressing cells are easily detected in the ORS of the growing follicles (arrows). g: Heparanase enzymatic activity in lysates of telogen (▲) and anagen (■) skin. Tissue lysates, prepared from skin samples collected on days 0 and 9 after depilation, were normalized for equal protein and incubated (24 hours, pH 6.0, 37°C) with sulfate-labeled ECM. Control ECM (◆) was incubated in reaction mixture without skin lysate. Labeled degradation fragments released into the incubation medium were analyzed by gel filtration on Sepharose 6B, as described in Materials and Methods. h, i: Heparanase promoter activation during depilation-induced hair cycle. The back skin of C57BL/6J mice was electroporated on day 2 after depilation (h) or day 5 (i) with CMV-LUC (top) and Hpse-LUC (bottom) reporter constructs. Forty-eight hours after reporter construct electroporation, light emission was monitored by a CCD camera, as described in Materials and Methods. Note that bioluminescent signal over the site of Hpse-LUC electroporation was detected on day 5 after depilation only, whereas over the site of CMV-LUC electroporation, signal was detected on both days 2 and 5 after depilation. Original magnifications: $\times 100$ (a–f); $\times 400$ (c, inset).

Course of Heparanase Promoter Activation during Depilation-Induced Hair Cycle

We next used an *in vivo* electroporation technique, to deliver the LUC reporter gene driven by heparanase promoter to the mouse back skin at different time points during the hair growth cycle. Recently, successful topical delivery of DNA to mouse skin has been reported, resulting in effective transfection of plasmid, primarily to the ORS-residing cells of the hair follicles.⁴³ By monitoring *in vivo* light emission with a CCD camera we tested whether heparanase induction occurs because of transcriptional activation of the heparanase gene. After depilation-induced synchronized hair cycling, the lower back skin of C57BL/6J mice was electroporated on days 2, 5, and 7 with a reporter construct containing the heparanase gene promoter region (1.9 kb) introduced in front of LUC reporter gene (Hpse-LUC).³⁸ This 1.9-kb region has

been previously shown to confer transcription promoter activity, enabling LUC expression in various cell lines transfected with the reporter construct (~500-fold increase versus cells transfected with basic plasmid alone).³⁸ As a positive control, CMV promoter-luciferase (CMV-LUC) construct was electroporated into a different site in the upper back skin of the same animals at the same time points. Forty-eight hours after reporter construct electroporation, light emission was monitored by a CCD camera. In mouse skin electroporated on day 2 after depilation, no bioluminescent emission was detected over the site of Hpse-LUC plasmid electroporation (Figure 1h). However, in mice electroporated on day 5 (Figure 1h) or day 7 (not shown) after depilation, light emission was readily detected in the site of Hpse-LUC plasmid electroporation. In contrast, at the site of control CMV-LUC plasmid electroporation, bioluminescent emission was detected in

mice electroporated on either days 2, 5, or 7, regardless of the time lapsed between depilation and plasmid electroporation (Figure 1, h and i), indicating that the differences in light emission obtained with Hpse-LUC plasmid were not because of variation in transfection efficiency. These data demonstrate that the increase in heparanase levels during anagen occurs through activation of heparanase gene promoter at a specific stage of the hair cycle.

Heparanase Is Expressed by Bulge Clonogenic Keratinocytes and Required for Their Migration in Vitro

To further investigate whether heparanase is specifically expressed by the migrating progeny of the bulge stem cells, we isolated clonogenic keratinocytes from the bulge region of the rat vibrissa ORS, where significant levels of the heparanase protein were detected by immunostaining (Figure 2a), similar to the mouse follicle. Hair follicle stem cell progeny have been previously identified as bulge-residing keratinocytes with a high *in vitro* clonogenic potential.^{5,7-9,32,44-46} Although hair follicle pluripotent bulge cells are not fully characterized in terms of specific markers, they preferentially express keratin 15 (K15).⁴⁵ The isolated keratinocytes from the rat vibrissa bulge region used in our experiments were highly clonogenic (Figure 2b), positive for K15 as well as for K5, K6, and K14 (Figure 2c), also known to be expressed by ORS bulge keratinocytes.⁴⁷ Furthermore, these cells lacked K10 (Figure 2c), a known early marker of terminal keratinocyte differentiation.^{6,47} Moreover, these cells, when cultured *in vitro*, moved with an average motility rate of 0.43 $\mu\text{m}/\text{minute}$, a typical mobility rate reported for epidermal stem cells and their daughter TA cells.⁴⁸ Based on these characteristics and on previous reports by Kobayashi and colleagues,³² and Oshima and colleagues,⁵ we conclude that the obtained cell population represents the immediate progeny of hair follicle stem cells.

We next tested whether heparanase contributes to the ability of clonogenic keratinocytes to penetrate ECM barriers during their downward migration from the bulge region. To mimic the *in vivo* conditions, we used the Matrigel migration/invasion assay,⁴⁹ previously applied to demonstrate the role of heparanase in facilitating cellular movement through ECM.²⁷ Bulge clonogenic keratinocytes were added to the upper compartment of 48-well Boyden chambers and allowed to migrate through porous polycarbonate membrane, coated with reconstituted basement membrane-like ECM (Matrigel), which closely resembles in this assay the naturally occurring ECM barrier for cell migration. The presence of laminaran sulfate, a potent inhibitor of heparanase enzymatic activity,⁵⁰ resulted in a significant and dose-dependent decrease in the ability of the bulge-derived clonogenic keratinocytes to pass through Matrigel-coated filters (Figure 2d). Similar results were obtained when a different heparanase-inhibiting compound (glycol split non-anticoagulant heparin)⁵¹ was used (not shown). In contrast,

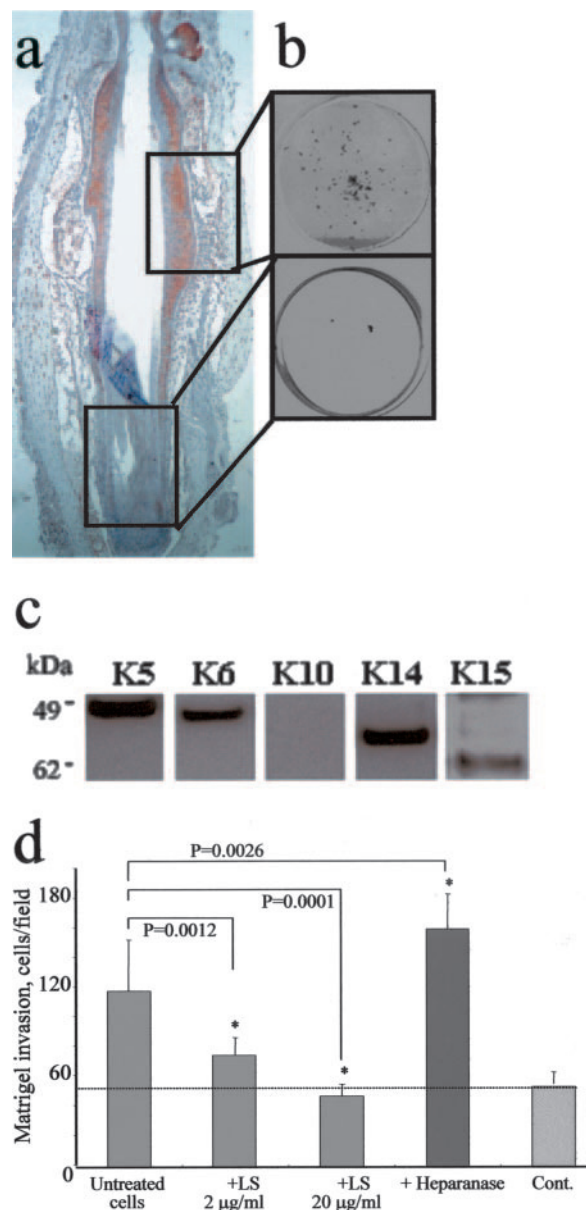


Figure 2. Heparanase is expressed by clonogenic keratinocytes from rat vibrissa bulge, representing hair stem cell population, and contributes to their migratory ability. **a:** Longitudinal section of a Fisher 344 rat vibrissa follicle, stained with anti-heparanase antibody (reddish staining). **b:** Cultured bulge keratinocytes were isolated from bulge region (top) or lower portion of ORS (bottom) of rat vibrissa follicles, fixed 9 days after isolation, and stained with crystal violet. Note that almost all colony-forming keratinocytes were derived from the bulge (heparanase-positive) portion, whereas little or no cell clones were obtained from the lower ORS region, which is heparanase-negative. **c:** After 9 days in culture, bulge clonogenic keratinocytes were washed with PBS and lysed in RIPA buffer. The lysates were analyzed by Western blot with antibodies against keratin (K) 5, 6, 10, 14, and 15, as described in Materials and Methods. Note the presence of epidermal stem cell marker K15 and absence of K10, which is an early marker of terminal differentiation. **d:** Invasion through Matrigel. Bulge clonogenic keratinocytes were added (30,000 cells/well, 6 hours, 37°C, 5% CO₂) on top of Matrigel-coated filters, and incubated in keratinocyte-SFM containing 1% bovine serum albumin. Some cells were also treated with either 2 $\mu\text{g}/\text{ml}$ or 20 $\mu\text{g}/\text{ml}$ of laminaran sulfate (+LS), or preincubated for 15 minutes with 5 $\mu\text{g}/\text{ml}$ of recombinant heparanase (+heparanase), followed by incubation on the top of the Matrigel-coated filters. The bottom chambers were filled with complete growth medium, containing epidermal growth factor (2.5 $\mu\text{g}/500$ ml), bovine pituitary extract (25 $\mu\text{g}/500$ ml), and 10% fetal calf serum. For a negative control (cont.), the bottom chamber was filled with keratinocyte-SFM. The number of cells/field on the lower surface of the filter was determined as described in Materials and Methods. Each data point represents the mean \pm SD of triplicate filters. Original magnification, $\times 50$ (a).

preincubation of the bulge clonogenic keratinocytes with recombinant heparanase (5 $\mu\text{g/ml}$) for 15 minutes before the assay facilitated cell movement across the Matrigel-coated filters (Figure 2d).

Increased Follicle Length, Dermal Thickness, and Anagen Duration during the First Postnatal Hair Cycle in *hpa*-Transgenic Mice

To investigate whether heparanase directly affects follicle cycling, we studied the physiological first postnatal hair cycle in heparanase-overexpressing transgenic mice (*hpa*-tg mice) expressing, among other tissues and organs, elevated levels of heparanase in follicular keratinocytes.³⁰ Skin samples derived from *hpa*-tg and control wild-type newborn mice were harvested on postnatal days 8, 12, 16, and 20, and evaluated for hair follicle development. As shown in Figure 3, a and b, histological analysis at postnatal day 8 revealed hair follicles in both control and *hpa*-tg mice at stage 6 to 7 of postnatal hair development, morphologically identical to anagen IV to V of later cycles,³⁵ indicating simultaneous initiation of the physiological first postnatal hair cycle in both types of mice. At postnatal day 16 (Figure 3, c and d), when the follicles of wild-type mice (Figure 3c) had already entered the early catagen phase (catagen III),³⁴ the majority of hair follicles in the *hpa*-tg mice (Figure 3d) were still actively growing (stage 8, identical to anagen VI).³⁵ On postnatal day 20, the majority of follicles in the control wild-type skin were scored as late catagen (catagen VII to VIII; Figure 3e), whereas in *hpa*-tg skin the follicles were at mid-catagen (Figure 3f). The prolonged active growth of *hpa*-tg follicles was reflected by a difference in skin thickness (Figure 3g), previously shown to correspond to the follicle length⁵² and the stage of hair cycle.^{22,34} No statistically significant difference in the cutaneous thickness (dermis + subcutis) of control wild-type versus *hpa*-tg skin was observed at postnatal day 8, further confirming concomitant initiation of follicular development in both these mice. However, on postnatal days 12, 16, and 20, a significant increase in cutaneous thickness was measured in the *hpa*-tg mice, as compared to their wild-type counterparts (Figure 3g). In addition, termination of the active phase of hair growth (reflected by the decrease in cutaneous thickness) was detected in wild-type but not in *hpa*-tg mice on postnatal day 16 indicating a delay of catagen onset in the transgenic skin. Similar differences in cutaneous thickness were observed during depilation-induced hair cycle in *hpa*-tg versus wild-type mice on days 8 (0.81 ± 0.06 mm versus 0.67 ± 0.07 mm, $P \leq 0.001$) and 13 (0.82 ± 0.03 mm versus 0.73 ± 0.06 mm, $P = 0.007$) after depilation (not shown).

Enhanced Hair Regrowth after Chemotherapy-Induced Hair Loss in *hpa*-tg Mice

The observed effects of heparanase on normal hair development and cycling led us to examine the conse-

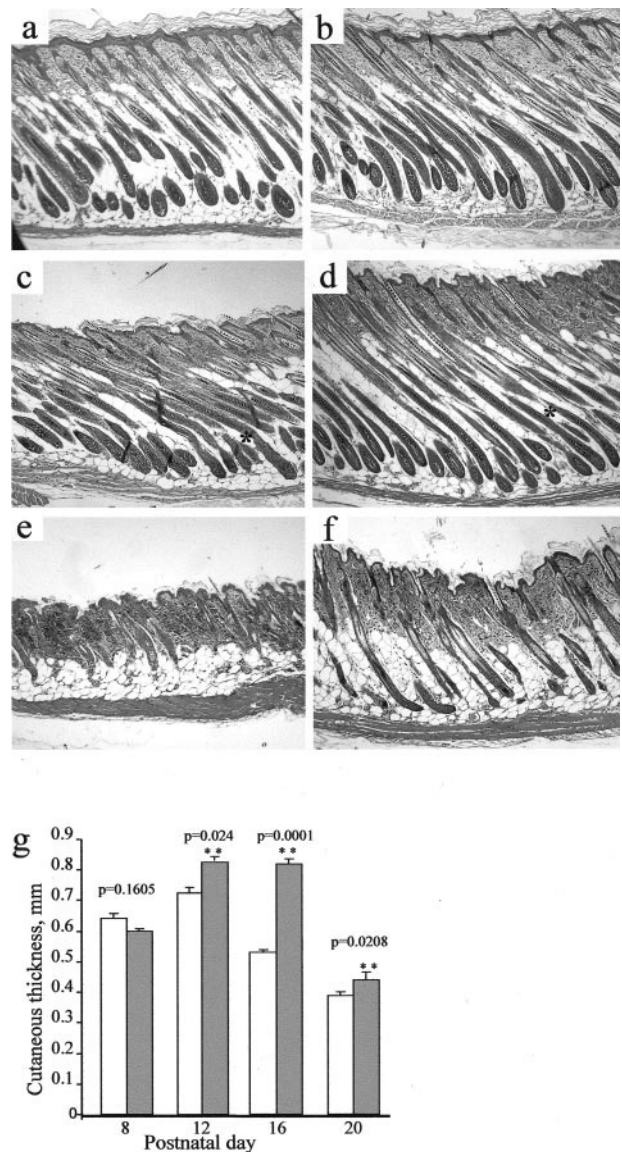


Figure 3. Course of the physiological first postnatal hair cycle in control wild-type and *hpa*-tg mouse skin. **a, b:** A representative skin section of control wild-type (**a**) and *hpa*-tg (**b**) mice at postnatal day (pd) 8, with the majority of follicles at stage 6 to 7 of postnatal morphogenesis, identical to anagen IV to V of subsequent cycles. **c, d:** On postnatal day 16, hair follicles of wild-type mice reached catagen III phase (**c**), while *hpa*-tg follicles (**d**) are actively growing (stage 6 to 7 of postnatal morphogenesis, corresponding to anagen VI of later cycles; asterisk designates a representative follicle in each stage). **e, f:** Skin section of wild-type (**e**) and *hpa*-tg (**f**) mice on postnatal day 20. Late catagen follicles (catagen VII to VIII) are mostly represented in wild-type skin (**e**), while mid-catagen follicles are observed in *hpa*-tg skin (**f**). **g:** Dermal thickness (dermis + subcutis) changes during the physiological first postnatal hair cycle in wild-type (open bars) and *hpa*-tg (filled bars) mice. H&E-stained sections were evaluated as described in Materials and Methods. Data are expressed as mean \pm SEM. The two-tailed P values were calculated using the t -test. Original magnifications, $\times 100$ (**a-f**).

quences of heparanase overexpression in an animal model of impaired hair growth. We used the cyclophosphamide (CYP)-induced alopecia model³⁶ to compare the rates of follicle recovery in *hpa*-tg versus control wild-type mice after hair loss in response to CYP chemotherapy. Administration of two repetitive doses of CYP to both *hpa*-tg and wild-type female mice resulted in severe hair loss on experimental day 15. A single dose administration

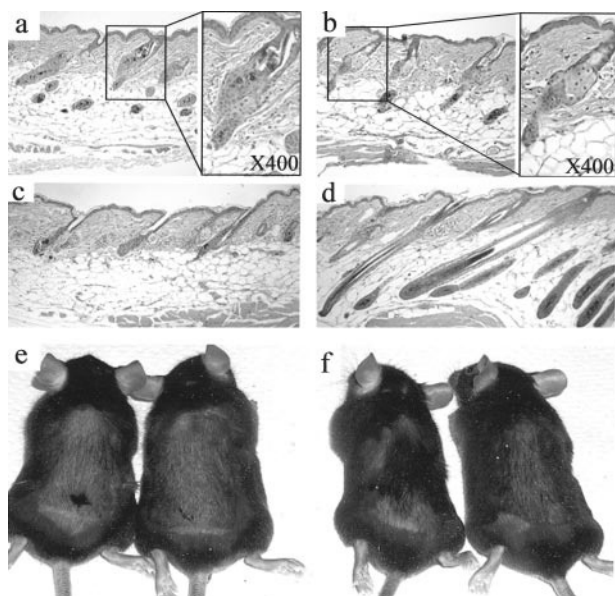


Figure 4. Accelerated hair regrowth in *hpa*-transgenic mice after chemotherapy-induced alopecia. Control wild-type and *hpa*-tg mice were depilated and treated with cyclophosphamide (CYP, two injections of 125 mg/kg body weight, on experimental days 1 and 3) to mimic a severe chemotherapy-induced alopecia. By experimental day 15, the mice in both wild-type (**a**) and *hpa*-tg (**b**) groups showed involution and regression of hair follicles, as revealed by histological examination of tissue sections. Macroscopically, complete alopecia on the dorsal skin was readily detected at that stage (not shown). On experimental day 30, intense hair regrowth was evident both by histology (**d**) and gross examination (**f**) in *hpa*-tg, but not control mice (**c**, **e**). Original magnifications, $\times 100$ (**a-d**).

of CYP produces two distinctive patterns of follicle damage: a mild form (dystrophic anagen) and a more severe response known as dystrophic catagen.³⁶ In our experiments, repeated administration of two consecutive doses of CYP resulted, as expected, in a significant increase in the relative percentage of dystrophic catagen follicles (Figure 4, a and b). Macro- and microscopic observations on experimental day 30 revealed restricted hair regrowth on wild-type mice skin (Figure 4e), probably because of a small fraction of the follicles that reached the active growth phase, while the majority of follicles were still in telogen (Figure 4c). By the same experimental day, a higher proportion of follicles have been actively growing in *hpa*-tg skin and a higher rate of hair growth recovery was observed (Figure 4, d and f). These data demonstrate that endogenously elevated levels of heparanase allow for a faster regrowth of hair in mice with chemotherapy-induced alopecia.

Discussion

The mammalian endoglycosidase heparanase is the predominant functional enzyme degrading heparan sulfate moieties, ubiquitously associated with the cell surface and ECM.^{10,25} This enzymatic activity is crucial for many fundamental biological processes that involve ECM disintegration, cell adhesion, and migration (ie, pregnancy, morphogenesis, inflammation, angiogenesis, cancer metastasis).^{10,17,25-28,30} Here, we show that heparanase is involved in hair follicle development and growth. Overex-

pression of heparanase in a mouse transgenic model enhanced both normal hair growth and recovery after chemotherapy-induced hair loss. We found that in C57/BL6 mice, expression and cellular distribution of endogenous heparanase through sequential phases of the hair growth cycle parallel the route and timing of TA cells (bulge-derived keratinocyte stem cell progeny) migration and reconstitution of the lower, cycling portion of the follicle.⁴ By monitoring *in vivo* activation of luciferase gene, driven by heparanase gene regulatory sequence, we demonstrated that the highly coordinated pattern of its expression occurs through activation of heparanase gene promoter at a specific stage of the hair cycle. Furthermore, we have shown that clonogenic keratinocytes isolated from the rat vibrissa bulge and closely related to the vibrissa follicle stem cell progeny,^{5,32} express heparanase when cultured *in vitro*. Treatment of these bulge-derived clonogenic keratinocytes with heparanase enzymatic inhibitors (laminaran sulfate, species of heparin) caused a dose-dependent decrease in their ability to traverse a layer of Matrigel (reconstituted ECM preparation), whereas preincubation with exogenous recombinant heparanase increased their migration through Matrigel. Interestingly, heparin, a powerful inhibitor of heparanase activity,⁵³ was reported to suppress the development of anagen follicles in mice,⁵⁴ although this effect was not attributed to the anti-heparanase properties of the compound. Moreover, our preliminary experiments demonstrate that local *in vivo* electroporation of anti-heparanase siRNA into the mouse skin markedly inhibited depilation-induced follicle activation (anagen), further corroborating the involvement of heparanase in hair growth.

Possible interpretation of the above data are that during active hair growth, heparanase contributes to the ability of TA cells to move through ECM barriers. Obviously, the migration of these cells along the ORS toward the bulb would require their release from adhesion sites and subsequent penetration of the ECM. Each of these processes is dependent, at least in part, on heparanase-mediated degradation of cell surface- and ECM-associated heparan sulfate.^{10,27} The importance of heparanase-mediated cleavage of extracellular heparan sulfate in hair biology may not be restricted merely to the removal of physical obstacles for cell migration. Several heparan sulfate-bound growth factors, implicated in hair growth and differentiation (ie, fibroblast growth factor, keratinocyte growth factor, vascular endothelial growth factor, and hepatocyte growth factor),^{2,22} are sequestered in the ECM and the basement membrane and could be released in an active form by means of enzymatic degradation of heparan sulfate.^{10,17,19,21,24} We have previously shown that heparanase releases heparan sulfate-bound basic fibroblast growth factor from ECM deposits, and at the same time generates bioactive heparan sulfate degradation fragments, potentiating the growth factor activity.^{10,28} This mode of action seems to be particularly relevant to explain the observed activation of hair regrowth in *hpa*-tg but not wild-type mice after CYP-induced alopecia. Expression of transgenic heparanase in this model is driven by a constitutive β -actin promoter³⁰

and therefore is not restricted to ORS keratinocytes during early-mid anagen, as shown for endogenous heparanase. In such a case the major contribution of heparanase to hair recovery may not be through facilitation of cell migration, but rather via enhanced release of ECM-sequestered, HS-bound growth factors regulating hair growth (keratinocyte growth factor, hepatocyte growth factor, and so forth) that may induce anagen earlier than in wild-type mice in which heparanase expression is restricted in time.

In the normally cycling follicle, heparanase expressed by TA cells that move downward and repopulate the lower follicle, may promote further TA cell proliferation and differentiation in a similar manner, via release of heparan sulfate-bound growth factors residing in the basement membrane that separates the epithelial core of the follicle from the mesenchymal elements (connective tissue sheath and dermal papilla).^{21,23,29} Finally, a recent report showed that improved follicle vascularization promotes hair growth,²² suggesting that part of the observed heparanase effects may also be attributed to its known proangiogenic activity.^{10,28} Although the above-mentioned mechanistic aspects are not fully elucidated, our results provide the first evidence for functional involvement of heparanase in hair follicle growth and encourage development of novel heparanase-based strategies for the treatment of hair growth disorders.

References

1. Paus R, Cotsarelis G: The biology of hair follicles. *N Engl J Med* 1999, 341:491–497
2. Stenn KS, Paus R: Controls of hair follicle cycling. *Physiol Rev* 2001, 81:449–494
3. Cotsarelis G, Sun TT, Lavker RM: Label-retaining cells reside in the bulge area of pilosebaceous unit: implications for follicular stem cells, hair cycle, and skin carcinogenesis. *Cell* 1990, 61:1329–1337
4. Taylor G, Lehrer MS, Jensen PJ, Sun TT, Lavker RM: Involvement of follicular stem cells in forming not only the follicle but also the epidermis. *Cell* 2000, 102:451–461
5. Oshima H, Rochat A, Kedzia C, Kobayashi K, Barrandon Y: Morphogenesis and renewal of hair follicles from adult multipotent stem cells. *Cell* 2001, 104:233–245
6. Janes SM, Lowell S, Hutter C: Epidermal stem cells. *J Pathol* 2002, 197:479–491
7. Wilson CL, Sun TT, Lavker RM: Cells in the bulge of the mouse telogen follicle give rise to the lower anagen follicle. *Skin Pharmacol* 1994, 7:8–11
8. Sun TT, Cotsarelis G, Lavker RM: Hair follicular stem cells: the bulge-activation hypothesis. *J Invest Dermatol* 1991, 96:77S–78S
9. Wilson C, Cotsarelis G, Wei ZG, Fryer E, Margolis-Fryer J, Ostead M, Tokarek R, Sun TT, Lavker RM: Cells within the bulge region of mouse hair follicle transiently proliferate during early anagen: heterogeneity and functional differences of various hair cycles. *Differentiation* 1994, 55:127–136
10. Vlodavsky I, Goldshmidt O, Zcharia E, Metzger S, Chajek-Shaul T, Atzmon R, Guatta-Rangini Z, Friedmann Y: Molecular properties and involvement of heparanase in cancer progression and normal development. *Biochimie* 2001, 83:831–839
11. Murphy G, Gavrilovic J: Proteolysis and cell migration: creating a path? *Curr Opin Cell Biol* 1999, 11:614–621
12. Lei TC, Vieira WD, Hearing VJ: In vitro migration of melanoblasts requires matrix metalloproteinase-2: implications to vitiligo therapy by photochemotherapy. *Pigment Cell Res* 2002, 15:426–432
13. Kjellen L, Lindahl U: Proteoglycans: structures and interactions [published erratum appears in *Annu Rev Biochem* 1992;61:following viii]. *Annu Rev Biochem* 1991, 60:443–475
14. Iozzo RV: Matrix proteoglycans: from molecular design to cellular function. *Annu Rev Biochem* 1998, 67:609–652
15. Nutbrown M, Randall VA: Differences between connective tissue-epithelial junctions in human skin and the anagen hair follicle. *J Invest Dermatol* 1995, 104:90–94
16. Jahoda CA, Mauger A, Bard S, Sengel P: Changes in fibronectin, laminin and type IV collagen distribution relate to basement membrane restructuring during the rat vibrissa follicle hair growth cycle. *J Anat* 1992, 181:47–60
17. Vlodavsky I: Involvement of the extracellular matrix, heparan sulphate proteoglycans, and heparan sulphate degrading enzymes in angiogenesis and metastasis. *Tumour Angiogenesis*. Edited by Lewis CE, Bicknell R, Ferrara N. Oxford, Oxford University Press, 1997, pp 125–140
18. Vlodavsky I, Bar-Shavit R, Kormer G, Fuks Z: Extracellular matrix-bound growth factors, enzymes and plasma proteins. *Basement Membranes: Cellular and Molecular Aspects*. Edited by Rohrbach DH, Timpl E. Orlando, Academic Press Inc., 1993, pp 327–343
19. Friedl A, Chang Z, Tierney A, Rapraeger AC: Differential binding of fibroblast growth factor-2 and -7 to basement membrane heparan sulfate: comparison of normal and abnormal human tissues. *Am J Pathol* 1997, 150:1443–1455
20. Folkman J, Klagsbrun M, Sasse J, Wadzinski M, Ingber D, Vlodavsky I: A heparin-binding angiogenic protein—basic fibroblast growth factor—is stored within basement membrane. *Am J Pathol* 1988, 130:393–400
21. Couchman JR, du Cros DL: Proteoglycans and associated proteins of the mammalian hair follicle. *J Invest Dermatol* 1995, 104:40S–41S
22. Yano K, Brown LF, Detmar M: Control of hair growth and follicle size by VEGF-mediated angiogenesis. *J Clin Invest* 2001, 107:409–417
23. du Cros DL, Isaacs K, Moore GP: Distribution of acidic and basic fibroblast growth factors in ovine skin during follicle morphogenesis. *J Cell Sci* 1993, 105:667–674
24. Masumoto A, Yamamoto N: Stimulation of DNA synthesis in hepatocytes by hepatocyte growth factor bound to extracellular matrix. *Biochem Biophys Res Commun* 1993, 191:1218–1223
25. Vlodavsky I, Friedmann Y, Elkin M, Aingorn H, Atzmon R, Ishai-Michaeli R, Bitan M, Pappo O, Peretz T, Michal I, Spector L, Pecker I: Mammalian heparanase: gene cloning, expression and function in tumor progression and metastasis. *Nat Med* 1999, 5:793–802
26. Parish CR, Freeman C, Hulett MD: Heparanase: a key enzyme involved in cell invasion. *Biochim Biophys Acta* 2001, 1471:M99–M108
27. Boyd DD, Nakajima M: Involvement of heparanase in tumor metastases: a new target in cancer therapy? *J Natl Cancer Inst* 2004, 96:1194–1195
28. Elkin M, Ilan N, Ishai-Michaeli R, Friedmann Y, Pappo O, Pecker I, Vlodavsky I: Heparanase as mediator of angiogenesis: mode of action. *FASEB J* 2001, 15:1661–1663
29. Couchman JR: Hair follicle proteoglycans. *J Invest Dermatol* 1993, 101:60S–64S
30. Zcharia E, Metzger S, Chajek-Shaul T, Aingorn H, Elkin M, Friedmann Y, Weinstein T, Li J-P, Lindahl U, Vlodavsky I: Transgenic expression of mammalian heparanase uncovers physiological functions of heparan sulfate in tissue morphogenesis, vascularization and feeding behavior. *FASEB* 2004, 18:252–263
31. Philip D, Nguyen M, Scheremeta B, St.-Surin S, Villa AM, Orgel A, Kleinman HK, Elkin M: Thymosin beta4 increases hair growth by activation of hair follicle stem cells. *FASEB J* 2004, 18:385–387
32. Kobayashi K, Rochat A, Barrandon Y: Segregation of keratinocyte colony-forming cells in the bulge of the rat vibrissa. *Proc Natl Acad Sci USA* 1993, 90:7391–7395
33. Paus R, Stenn KS, Link RE: Telogen skin contains an inhibitor of hair growth. *Br J Dermatol* 1990, 122:777–784
34. Muller-Rover S, Handjiski B, van der Veen C, Eichmuller S, Foitzik K, McKay IA, Stenn KS, Paus R: A comprehensive guide for the accurate classification of murine hair follicles in distinct hair cycle stages. *J Invest Dermatol* 2001, 117:3–15
35. Paus R, Muller-Rover S, Van Der Veen C, Maurer M, Eichmuller S, Ling G, Hofmann U, Foitzik K, Mecklenburg L, Handjiski B: A comprehensive guide for the recognition and classification of distinct stages of hair follicle morphogenesis. *J Invest Dermatol* 1999, 113:523–532

36. Paus R, Handjiski B, Eichmuller S, Czarnetzki BM: Chemotherapy-induced alopecia in mice. Induction by cyclophosphamide, inhibition by cyclosporine A, and modulation by dexamethasone. *Am J Pathol* 1994, 144:719–734
37. Zetser A, Levi-Adam F, Kaplan V, Gingis-Velitsky S, Bashenko Y, Schubert S, Flugelman MY, Vlodaysky I, Ilan N: Processing and activation of latent heparanase occurs in lysosomes. *J Cell Sci* 2004, 117:2249–2258
38. Elkin M, Cohen I, Zcharia E, Orgel A, Guatta-Rangini Z, Peretz T, Vlodaysky I, Kleinman HK: Regulation of heparanase gene expression by estrogen in breast cancer. *Cancer Res* 2003, 63:8821–8826
39. Zhang L, Nolan E, Kreitschitz S, Rabussay DP: Enhanced delivery of naked DNA to the skin by non-invasive in vivo electroporation. *Biochim Biophys Acta* 2002, 1572:1–9
40. Honigman A, Zeira E, Ohana P, Abramovitz R, Tavor E, Bar I, Zilberman Y, Rabinovsky R, Gazit D, Joseph A, Panet A, Shai E, Palmon A, Laster M, Galun E: Imaging transgene expression in live animals. *Mol Ther* 2001, 4:239–249
41. Vlodaysky I, Fuks Z, Bar-Ner M, Ariav Y, Schirrmacher V: Lymphoma cell-mediated degradation of sulfated proteoglycans in the subendothelial extracellular matrix: relationship to tumor cell metastasis. *Cancer Res* 1983, 43:2704–2711
42. Vlodaysky I, Eldor A, Haimovitz-Friedman A, Matzner Y, Ishai-Michaeli R, Lider O, Naparstek Y, Cohen IR, Fuks Z: Expression of heparanase by platelets and circulating cells of the immune system: possible involvement in diapedesis and extravasation. *Invasion Metastasis* 1992, 12:112–127
43. Domashenko A, Gupta S, Cotsarelis G: Efficient delivery of transgenes to human hair follicle progenitor cells using topical lipoplex. *Nature Biotechnol* 2000, 18:420–423
44. Rochat A, Kobayashi K, Barrandon Y: Location of stem cells of human hair follicles by clonal analysis. *Cell* 1994, 76:1063–1073
45. Lyle S, Christofidou-Solomidou M, Liu Y, Elder DE, Albelda S, Cotsarelis G: The C8/144B monoclonal antibody recognizes cytokeratin 15 and defines the location of human hair follicle stem cells. *J Cell Sci* 1998, 111:3179–3188
46. Barrandon Y, Green H: Three clonal types of keratinocyte with different capacities for multiplication. *Proc Natl Acad Sci USA* 1987, 84:2302–2306
47. Fuchs E: Keratins and the skin. *Annu Rev Cell Dev Biol* 1995, 11:123–153
48. Jensen UB, Lowell S, Watt FM: The spatial relationship between stem cells and their progeny in the basal layer of human epidermis: a new view based on whole-mount labelling and lineage analysis. *Development* 1999, 126:2409–2418
49. Albin A, Iwamoto Y, Kleinman HK, Martin GR, Aaronson SA, Kozlowski JM, McEwan RN: A rapid in vitro assay for quantitating the invasive potential of tumor cells. *Cancer Res* 1987, 47:3239–3245
50. Miao HQ, Elkin M, Aingorn E, Ishai-Michaeli R, Stein CA, Vlodaysky I: Inhibition of heparanase activity and tumor metastasis by laminarin sulfate and synthetic phosphorothioate oligodeoxynucleotides. *Int J Cancer* 1999, 83:424–431
51. Naggi A, Casu B, Perez M, Torri G, Cassinelli G, Penco S, Pisano C, Giannini G, Ishai-Michaeli R, Vlodaysky I: Modulation of the heparanase-inhibiting activity of heparin through selective desulfation, graded N-acetylation, and glycol-splitting. *J Biol Chem* 2005, Jan 12 (online)
52. Andreasen E: Cyclic changes in the skin of the mouse. *Acta Pathol Microbiol Scand* 1953, 32:157–164
53. Bar-Ner M, Eldor A, Wasserman L, Matzner Y, Cohen IR, Fuks Z, Vlodaysky I: Inhibition of heparanase-mediated degradation of extracellular matrix heparan sulfate by non-anticoagulant heparin species. *Blood* 1987, 70:551–557
54. Paus R: Hair growth inhibition by heparin in mice: a model system for studying the modulation of epithelial cell growth by glycosaminoglycans? *Br J Dermatol* 1991, 124:415–422